

Electrochemical and Theoretical Investigation of Triazole Derivatives as Corrosion Inhibitors for Copper in 3.5% NaCl Solution

Huiwen Tian, Weihua Li^{*}, Baorong Hou

Key Laboratory of Corrosion Science, Shandong, Institute of Oceanology, Chinese Academy of Sciences, Qingdao 266071, China

*E-mail: liweihua@qdio.ac.cn

Received: 25 November 2012 / Accepted: 29 April 2013 / Published: 1 June 2013

This paper presents the investigation of 4-amino-5-phenyl-4H-1,2,4-triazole-3-thiol and 4-amino-5-nitrophenyl-4H-1,2,4-triazole-3-thiol as corrosion inhibitors for copper in 3.5% NaCl solution. Determinations of weight loss, electrochemical measurements, scanning electronic microscope (SEM) and quantum chemical calculation were performed to analyze the inhibiting performance of these compounds. All compounds showed >90% inhibition efficiency at their optimum concentration. Thermodynamic calculation suggests that the adsorption of the inhibitors was found to follow the Langmuir adsorption isotherm. The relationships between inhibition efficiency and the molecular orbitals were calculated by quantum chemical method. The inhibition efficiency increased with the increase in E_{HOMO} and decrease in $E_{\text{LUMO}}-E_{\text{HOMO}}$.

Keywords: Copper; EIS; Polarization; SEM; Neutral inhibitor

1. INTRODUCTION

Using the marine resources is an effective way to relieve the resource shortage problem around the world. Seawater is often used as raw material instead of freshwater, the fluid, and operating medium in many fields. Copper has been one of more important materials in industry owing to its high electrical and thermal conductivities, excellent workability, it has widely used in the condenser pipe of various ships, the coast power plant heat exchangers and so on. While, the high concentration of Cl^- in seawater causes serious corrosion of copper and its alloys [1-3]. Hence, this inspires scientists to develop various methods to control the corrosion of copper in the marine environment, which can increase absolutely the service lifetime of copper and reduces the economic losses.

Employment of organic derivatives as inhibitors in the protection of metals and their alloys from seawater corrosion is one of effectively important method [4,5] due to the predominance in their chemical structures and properties, such as containing polar groups, conjugated double bonds or various heteroatoms—sulphur, nitrogen and oxygen [6-8]. For instance, benzotriazole (BTA) and its derivatives are often employed to protect copper and its alloys from corrosion. While owing to the toxicity of BTA and its derivatives to environments [9-11], the extensive studies have been performed to look for new environment-friendly organic inhibitors in recent decades, including triazole derivatives [12,13], tetrazole derivatives [14], thiadiazole derivatives [15], cysteine [16], substituted uracils [17], imidazole derivatives [18] and so on.

The aim of this work is to study the effect of 4-amino-5-phenyl-4H-1,2,4-triazole-3-thiol (APTT) and 4-amino-5-nitrophenyl-4H-1,2,4-triazole-3-thiol (ANTT) as corrosion inhibitors on the corrosion inhibition of copper in 3.5% NaCl solution. The performance of the compounds has been evaluated by weight loss, polarization curves, the electrochemical impedance spectroscopy (EIS), scanning electronic microscope (SEM) and energy dispersive X-ray spectroscopy (EDX). In addition, we investigate the adsorption mechanism of these inhibitors on copper surface by using Langmuir isotherm and quantum chemical method.

2. EXPERIMENTAL

2.1 Materials and sample preparation

The molecular structures of the studied compounds, namely 4-amino-5-phenyl-4H-1,2,4-triazole-3-thiol (APTT) and 4-amino-5-nitrophenyl-4H-1,2,4-triazole-3-thiol (ANTT), were shown in Fig. 1.

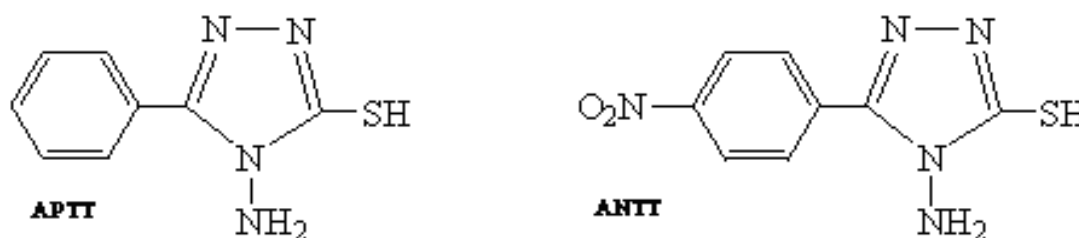


Figure 1. The structure of APTT and ANTT

The copper specimens (99.99%) for electrochemical experiments were embedded in epoxy resin with a geometrical surface area of 1 cm² exposed to the electrolyte. Prior to all measurements, the samples were abraded with emery paper from 600, 800, 1000, 2000 grit, respectively, degreased ultrasonically in ethanol, and dried at room temperature.

The concentration range of the inhibitors was from 5 to 100 mg/L in 3.5% NaCl solution. The solution in the absence of inhibitors was taken as blank for comparison.

2.2 Electrochemical experiment

The electrochemical measurements were conducted with PARSTAT 2273 Potentiostat/Galvanostat (Princeton Applied Research) in a conventional three-electrode cell system. A freshly abraded copper specimen and a platinum electrode were used as working electrode and counter electrode, respectively. A saturated calomel electrode (SCE) with a Luggin capillary was used as reference electrode. All potentials were measured versus SCE and tests were performed in non-deaerated solution at 303 K.

Electrochemical impedance spectroscopy (EIS) measurements were carried out at the open circuit potential (OCP). The ac frequency range extended from 100 kHz to 10 mHz with a 10 mV peak-to-peak sine wave as the excitation signal. The impedance data were analyzed and fitted with ZSimpWin ver. 3.21.

The polarization curves were obtained from -250 to +250 mV (versus OCP) with 0.5 mV/s scan rate, and the data were collected and analyzed by electrochemical software PowerSuite ver. 2.58.

2.3 Weight loss

Copper specimens in triplicate were immersed in the test NaCl solution for 14 days under each condition. After that, the specimens were removed from the solution, rinsed in 3.5% NaCl solution, water and acetone, finally dried and weighted. Weight loss experiments were used to calculate the mean corrosion rate (W , g cm⁻² h⁻¹). The inhibition efficiency was evaluated by Eq.(1)

$$IE (\%) = \frac{W_0 - W}{W_0} \times 100 \quad (1)$$

where W_0/W was the corrosion rate of copper in the solution without/with the inhibitor.

2.4 Surface analysis

The surface morphology of the specimens after immersing in 3.5% NaCl solution with and without inhibitors was performed on a scanning electronic microscope (SEM) and energy dispersive X-ray spectroscopy (EDX). The accelerating voltage was 20 kV.

2.5 Quantum chemical calculation

In order to find out optimized conformations of the compounds studied and to speed up the calculations, the molecular structures were optimized initially with PM3 semi-empirical calculation. The convergence was set to 4.184 J / mol.

3. RESULTS AND DISCUSSION

3.1 Polarization curves

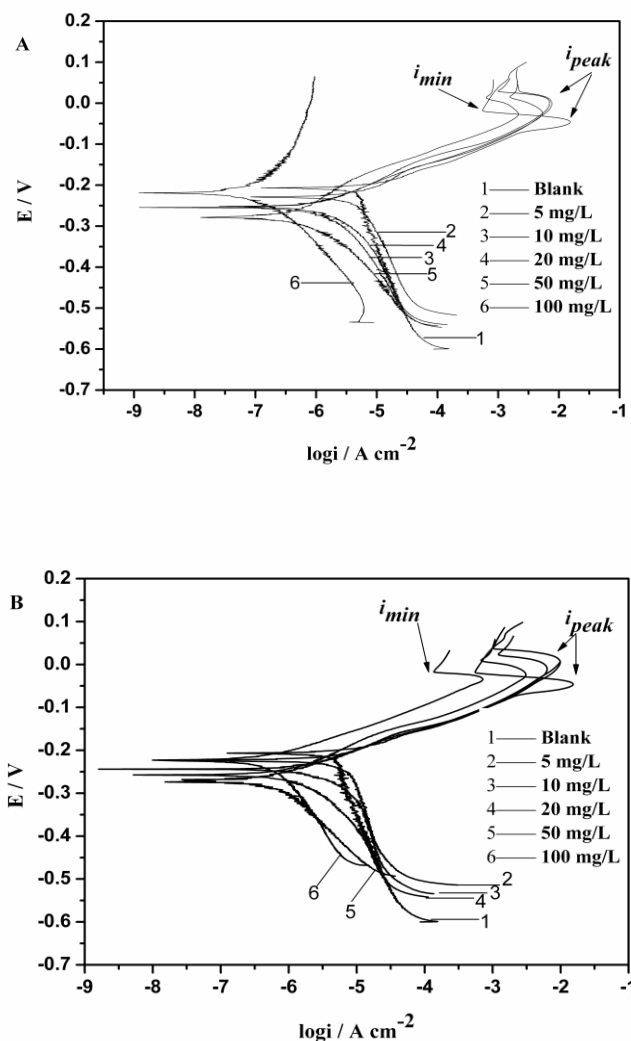


Figure 2. Polarization curves of copper in 3.5% NaCl solution with different concentrations of inhibitors: (A) APTT; (B) ANTT.

In order to understand the mechanism about the protection observed, the polarization curves of copper in 3.5% NaCl solution without and with different concentrations of APTT and ANTT are shown in Fig. 2.

The anodic and cathodic current-potential curves are extrapolated up to their intersection at a point where corrosion current density (i_{corr}) and corrosion potential (E_{corr}) are obtained [19]. The electrochemical parameters such as E_{corr} , i_{corr} , anodic and cathodic Tafel slopes (β_a , β_c) obtained from polarization measurements are listed in Table 1. The inhibition efficiency was calculated using Eq.(2)

$$IE_i(\%) = \frac{i_{0,corr} - i_{corr}}{i_{0,corr}} \times 100 \quad (2)$$

where i_{corr} and $i_{0,corr}$ are the corrosion current density of copper with and without inhibitors in 3.5% NaCl solution, respectively.

Table 1. Corrosion parameters of copper in 3.5% NaCl with different concentration of inhibitors at 303 K.

Concentration (mg/L)	i_{corr} ($\mu\text{A cm}^{-2}$)	E_{corr} (mV/SCE)	β_c (mV dec^{-1})	β_a (mV dec^{-1})	IE (%)
Blank	4.52	-218	177.2	47.6	—
APTT					
5	2.84	-240	90.5	56.3	37.1
10	0.86	-252	87.7	58.2	80.9
20	0.83	-250	72.4	53.7	81.6
50	0.35	-279	59.8	85.8	92.3
100	0.22	-225	97.9	76.2	95.1
ANTT					
5	2.90	-241	45.2	45.1	35.9
10	1.79	-246	74.9	58.7	60.3
20	0.87	-263	89.1	54.7	80.9
50	0.77	-247	68.2	54.2	83.1
100	0.40	-224	67.3	52.0	91.2

In Fig. 2, it can be seen that the anodic and cathodic current density in solution using APTT and ANTT have lower values compared with that of the blank solution. The shift of the cathodic Tafel slope β_c indicates that the oxygen reduction is restrained in the presence of the inhibitors. From the anodic polarization curves in Fig. 2, it shows that the peak current density disappears or decreases greatly. It is likely that the inhibitor molecules have adsorbed onto the copper surface, which could decrease the oxidation rate of Cu (0) to Cu (I) [20]. Therefore, it might be difficult for the corrosion to proceed to the next step.

In Table 1, we see the corrosion current density (i_{corr}) decreases greatly as APTT and ANTT are added into the solution. The inhibition efficiencies obtained from the polarization curves increase with the compounds concentration. The obtained values with APTT are larger than those with ANTT. The maximum value of inhibition efficiency is 95.1% with APTT and 91.2% with ANTT at 100 mg/L concentration. Together with other parameters, such as the corrosion potential (E_{corr}) decreasing slightly with the addition of APTT and ANTT, and the displacements are less than 85 mV/SCE. Thus it shows that both compounds act as the mixed-type corrosion inhibitors [21] which suppress both anodic and cathodic reaction by adsorbing on the copper surface. Fig. 2 further reveals that the cathodic suppression plays a dominant role in this process.

3.2 Electrochemical Impedance Spectroscopy (EIS)

Nyquist plots in the presence and absence of APTT and ANTT are given in Fig. 3. The plots show several convex arcs and each diameter of the arcs increases with the inhibitor concentration. It indicates that the impedance values have increased and the copper has gotten more protection.

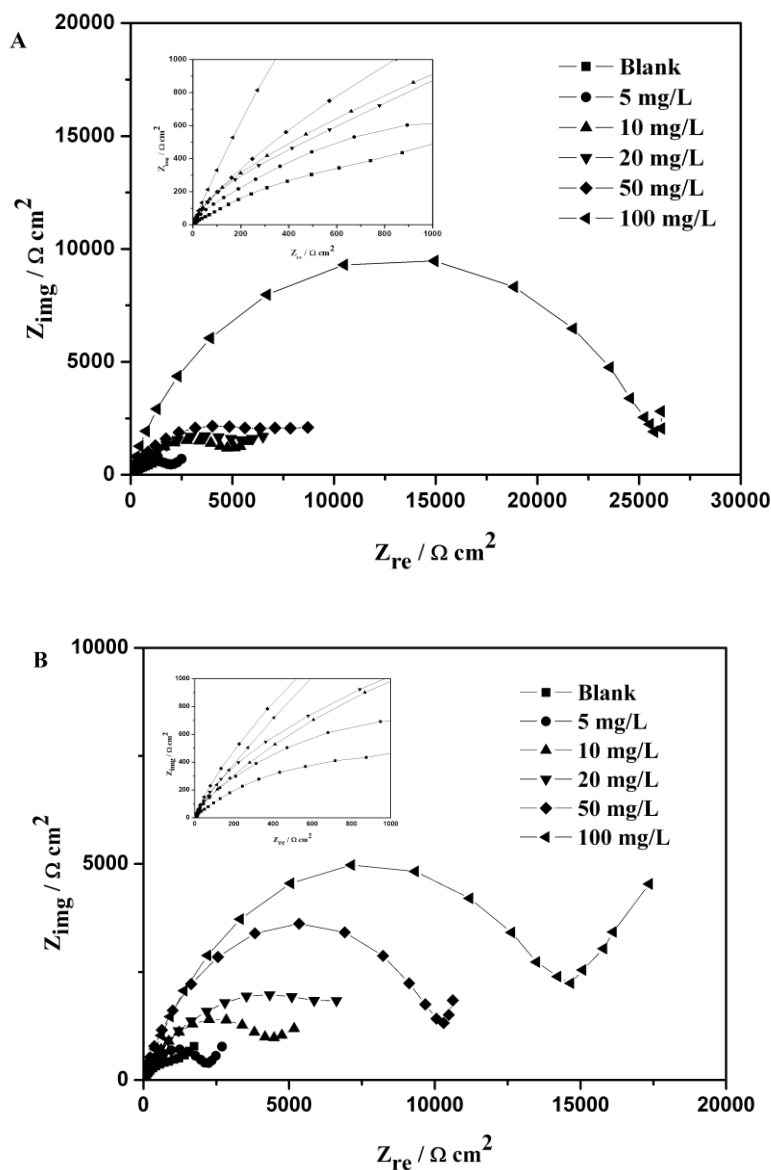


Figure 3. Nyquist plots for copper in 3.5% NaCl solution with different concentrations of inhibitors at 303 K: (A) APTT; (B) ANTT.

The equivalent circuit model used to fit the experimental results is shown in Fig. 4. R_s is the resistance of the solution between the working electrode and the reference electrode. R_f is the resistance of the film formed on the copper surface. R_{ct} represents the charge-transfer resistance. Constant phase element Q_I is composed of the membrane capacitance CPE_f and the deviation

parameter n_1 , and Q_2 is composed of the double-layer capacitance CPE_{dl} and the deviation parameter n_2 .

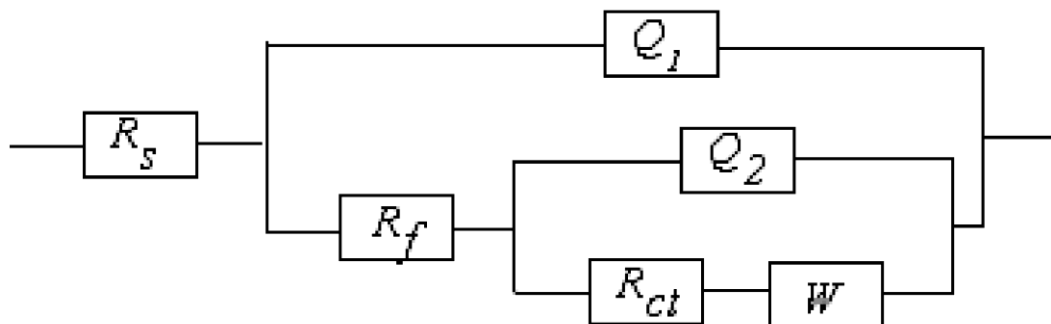


Figure 4. The equivalent circuit model used to fit the EIS experiment data.

The impedance of CPE is expressed as

$$Z_{CPE} = \frac{1}{Y(j\omega)^n} \quad (3)$$

where Y is a proportional factor, ω is the angular frequency, and n is the deviation parameter.

Table 2. Impedance parameters of copper in 3.5% NaCl solution with different concentrations of inhibitors at 303 K.

Concentration (mg/L)	R_s ($\Omega \text{ cm}^2$)	CPE_f ($\mu\text{F cm}^{-2}$)	n_1	CPE_{dl} ($\mu\text{F cm}^{-2}$)	n_2	R_f ($\Omega \text{ cm}^2$)	R_{ct} ($\Omega \text{ cm}^2$)	W	IE (%)
Blank	1.30	247	1	475	0.57	45.31	1109	5.06×10^{-3}	—
APTT									
5	2.87	14.7	1	144	0.53	200.2	2483	7.60×10^{-3}	55.3
10	2.42	12.0	1	98.3	0.57	450.2	5049	2.80×10^{-3}	78.1
20	1.35	12.8	0.99	88.2	0.55	452.6	6510	3.24×10^{-3}	82.9
50	1.18	4.56	1	8.50	0.57	460.9	8258	1.95×10^{-3}	86.6
100	0.89	4.32	0.99	4.72	0.74	1979	23300	7.08×10^{-4}	95.3
ANTT									
5	2.68	126	1	117	0.60	125.7	2324	5.34×10^{-3}	52.3
10	4.58	27.0	0.96	99.3	0.62	453.9	4199	3.34×10^{-3}	73.6
20	3.91	25.7	0.95	62.4	0.78	465.9	8704	2.94×10^{-3}	87.3
50	1.29	20.8	1	9.42	0.58	474.6	10090	1.65×10^{-3}	89.0
100	2.69	13.2	0.99	0.93	0.58	1278	13030	1.32×10^{-3}	91.5

According to the equivalent circuit, the impedance data are fitted and the electrochemical parameters are given in Table 2. The inhibition efficiency (IE) with APTT and ANTT in different concentrations is calculated by

$$IE_R(\%) = \frac{R_{ct} - R_{0,ct}}{R_{ct}} \times 100 \quad (4)$$

where R_{ct} and $R_{0,ct}$ represent the resistance of charge transfer in the presence and absence of inhibitors, respectively.

As shown in Table 2, the addition of APTT and ANTT increases the R_{ct} values and this effect seems to be enhanced upon the increasing of the inhibitor concentration. IE values reach the maximum 95.3% and 91.5% at 100 mg/L concentration, respectively. Thus, in order to prevent copper from the corrosion of Cl^- , the charge transfer process has been greatly inhibited by the inhibitors. Compared with the blank, the values of R_f with the inhibitors also increase obviously, which reveals that a more protective adsorption film is formed on copper surface.

It is also shown in Table 2 that the CPE_{dl} values decrease with the increasing of inhibitor concentration. That is due to the gradual replacement of water molecules by the adsorption of the organic molecules at metal/solution interface, which leads to a protective film adsorbing on the metal surface [22]. CPE_{dl} is expressed as

$$CPE_{dl} = \frac{\varepsilon^0 \varepsilon}{d} S \quad (5)$$

where d is the thickness of the film, S is the surface of the electrode, ε^0 is the permittivity of the air, and ε is the local dielectric constant. According to Eq. 5, the decrease in CPE_{dl} can be explained by either the increase in the adsorption film area (which decreases the electrode surface area), the decrease in the local dielectric constant or the increase in the double layer thickness. Therefore, the diffusion of ions from the interface to the solution may be delayed and the dissolution reactions of copper may be inhibited to a great extent.

3.3 Weigh loss measurement

3.3.1 Effect of inhibitor concentration

The effect of addition of different inhibitors at various concentrations on the copper corrosion in 3.5% NaCl solution was studied by weight loss measurement at 303 K after 14 d immersion. The values of inhibition efficiency and corrosion rate obtained from weight loss measurement are listed in Table 3. The corrosion rate values ($\text{mg cm}^{-2} \text{h}^{-1}$) of copper in 3.5% NaCl solution decrease as the concentration of inhibitor increase. The results show that the inhibition efficiency increases as the concentration of the inhibitor increases from 5 to 100 mg/L. The maximum inhibition efficiency was about 92% at 100 mg/L for APTT. From Table 3, it is clear that the order of inhibition efficiency of inhibitors as follows: ANTT < APTT.

Table 3. Corrosion parameters obtained from weight loss measurements for copper in 3.5% NaCl containing various concentrations of inhibitors at 303 K.

Inhibitors	Concentration (mg L ⁻¹)	C_R (mg cm ⁻² h ⁻¹)	θ	IE (%)
blank	0	7.11	—	—
APTT	5	3.56	0.499	49.9
	10	1.34	0.812	81.2
	20	1.22	0.828	82.8
	50	0.75	0.895	89.5
	100	0.57	0.920	92.0
ANTT	5	3.79	0.467	46.7
	10	2.41	0.661	66.1
	20	1.52	0.786	78.6
	50	1.04	0.854	85.4
	100	0.63	0.911	91.1

3.3.2 Effect of temperature

Table 4. Corrosion parameters obtained from weight loss measurements for copper in 3.5% NaCl in absence and presence of 100 mg/L inhibitors at different temperature.

Inhibitors	Temperature (K)	C_R (mg cm ⁻² h ⁻¹)	IE (%)
blank	303	7.11	—
	313	9.77	—
	323	14.7	—
	333	18.8	—
APTT	303	0.57	92.0
	313	1.12	88.5
	323	2.37	83.9
	333	4.21	77.6
ANTT	303	0.63	91.1
	313	1.23	87.4
	323	2.19	85.1
	333	3.73	80.1

Weight loss measurements were taken at various temperatures (303~333 K) in the absence and presence of inhibitors (100 mg/L) for 14 d of immersion in 3.5% NaCl solution. The corresponding inhibition efficiency (IE) is summarized in Table 4. The corrosion rate increases with the rise of temperature. The inhibition efficiencies are found to decrease with increasing the solution temperature from 303 to 333 K. The decrease in inhibition efficiencies might be due to the weakening of adsorbed inhibitor film on the copper surface.

3.3.3 Adsorption isotherm

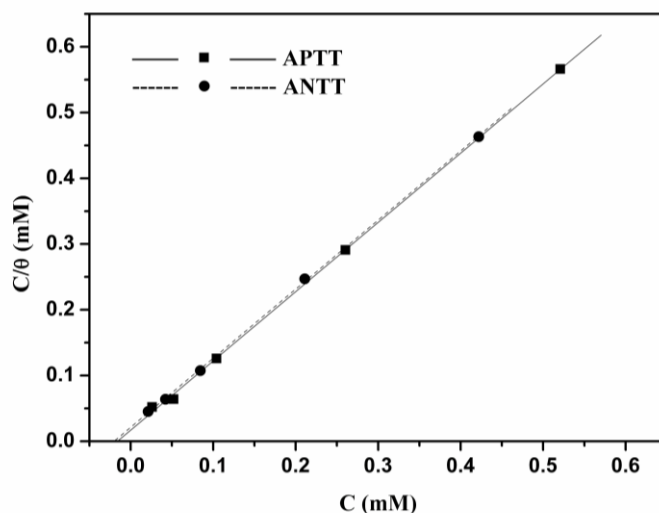


Figure 5. Langmuir's isotherm plots for adsorption of APTT and ANTT on copper

It is known that the adsorption isotherm is an effective way to explain the adsorption mechanism of the inhibitors. The interaction between the organic molecules and the metal surface could also be found in this method. Results obtained from weigh loss method are used to study the adsorption of APTT and ANTT on the copper surface. The surface coverage, θ , was calculated according to the following equation:

$$\theta = \frac{C_{0,R} - C_R}{C_{0,R}} \quad (6)$$

where, $C_{0,R}$ and C_R are the corrosion rates of copper for uninhibited and inhibited solutions, respectively.

In order to determine the best fit for θ to various isotherms, several adsorption isotherms are considered, such as Temkin, Langmuir, Frumkin and Freundlich isotherms:

$$\text{Temkin isotherm: } \exp(f \cdot \theta) = K_{ads} \cdot C \quad (7)$$

$$\text{Langmuir isotherm: } (\theta/1-\theta) = K_{ads} \cdot C \quad (8)$$

$$\text{Frumkin isotherm: } \frac{\theta}{n(1-\theta)^n} \exp(-2f\theta) = K_{ads} \cdot C \quad (9)$$

$$\text{Freundlich isotherm: } \theta = K_{ads} \cdot C \quad (10)$$

where K_{ads} is the equilibrium constant for adsorption process, C is the concentration of inhibitor and f is the energetic inhomogeneity. By far the best fit is obtained with the Langmuir adsorption isotherm. The plot of C/θ vs. C gave a straight line as shown in Fig.5.

3.3.4. Thermodynamic activation parameters

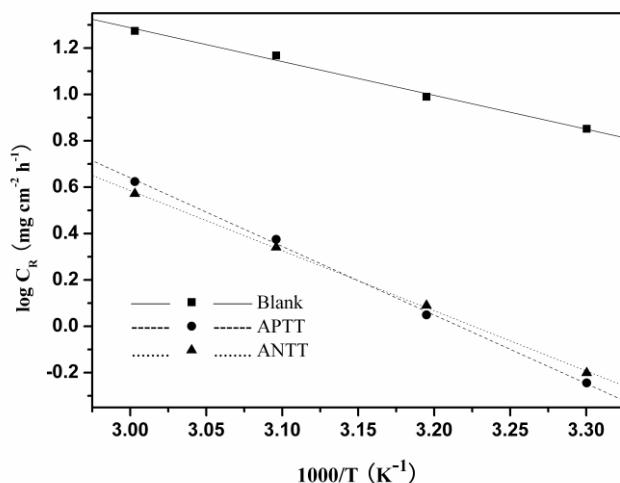


Figure 6. Arrhenius polts of log CR vs. 1000/T for copper in 3.5% NaCl without and with inhibitors

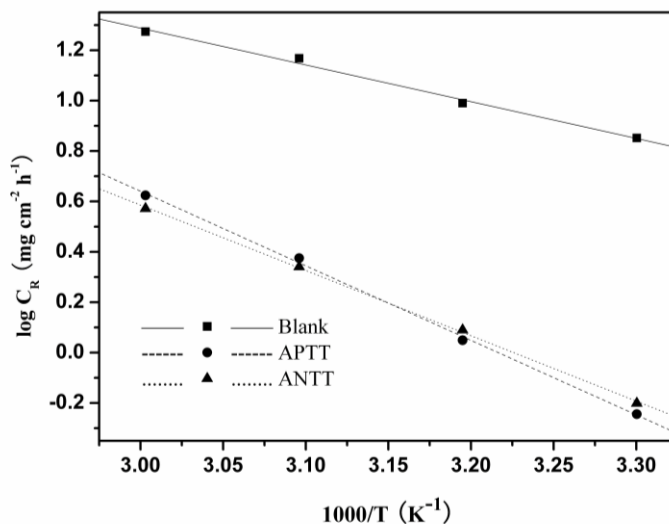


Figure 7. Arrhenius polts of log CR/T vs. 1000/T for copper in 3.5% NaCl without and with inhibitors

The dependence of corrosion rate at temperature can be expressed by Arrhenius equation and transition state equation:

$$\log(C_R) = \frac{-E_a}{2.303RT} + \lambda \tag{11}$$

$$C_R = \frac{RT}{Nh} \exp\left(\frac{\Delta S^*}{R}\right) \exp\left(-\frac{\Delta H^*}{RT}\right) \quad (12)$$

where E_a is the apparent effective activation energy, R is the general gas constant, T is the temperature, λ is the Arrhenius pre-exponential factor, h is the Plank constant, N is the Avogadro number, ΔS^* is the entropy of activation and ΔH^* is the enthalpy of activation.

Table 5. Activation parameters for copper in 3.5% NaCl solution obtained from weight loss measurement.

Inhibitors	ΔG_{ads}^0 (kJ mol ⁻¹)	E_a (kJ mol ⁻¹)	ΔH^* (kJ mol ⁻¹)	ΔS^* (J mol ⁻¹ K ⁻¹)
Blank	—	27.9	25.3	-145.3
APTT	-37.8	56.6	54.0	-71.6
ANTT	-37.2	49.7	47.0	-93.6

A plot of $\log C_R$ vs. $1000/T$ gave straight line as shown in Fig.6. The values of activation energy obtained from the slope of the lines are listed in Table 5. Fig.7 showed the plot of $\log C_R/T$ vs. $1000/T$. Straight lines were obtained with a slope of $(\Delta H^*/R)$, and an intercept of $[(\log(R/Nh))(\Delta S^*/R)]/2.303$ from which the values of ΔH^* and ΔS^* have been calculated and listed in Table 5. Inspection of Table 5 showed that the values of E_a determined in solution containing inhibitors are higher than that of in absence. The increase in E_a may be resulted either due to physical adsorption or due to decrease in the adsorption of inhibitor molecules on the copper surface with increase in temperature [23]. Positive sign of ΔH^* reflected the endothermic nature of copper dissolution process, which suggested the slow dissolution of copper [24]. As for the values of ΔS^* concern, the negative value is obtained in case of APTT, ANTT and uninhibited 3.5% NaCl solution. These variations are observed due to ordering and disordering of the inhibitor molecules on the metal surface [25]. The adsorption of organic inhibitor molecules in aqueous phase to metal surface can be regarded as quasi-substitution process between the organic molecules in the aqueous phase and water molecules on the metal surface [26]. The adsorption of inhibitors on copper surface would be in equilibrium with desorption of water molecules from the surface:



The adsorption process for the inhibitor is believed to be exothermic and accompanied with the decrease in entropy of the solute and increase in entropy of the solvent. The thermodynamic values obtained for entropy of activation are the algebraic sum of the adsorption of organic molecules (solute) and desorption of water (solvent) molecules [27], hence, the increase in entropy is attributed to increase in solvent entropy [28].

The standard free energy of adsorption ΔG_{ads} is related to adsorption constant (K_{ads}) with following equation [29]:

$$\Delta G_{ads}^0 = -\frac{RT}{2.303} \log(55.5K_{ads}) \quad (14)$$

The value 55.5 is the concentration of water in solution expressed in mol/L [30]. The values of ΔG_{ads} and K_{ads} are listed in Table 5. The negative values of ΔG_{ads} ensure the spontaneity of the adsorption process and stability of the adsorbed layer on the metal surface [31]. Generally, the values of ΔG_{ads} up to 20 kJ/mol are consistent with the electrostatic interaction (physisorption) of charged molecules with charged metal, while those around 40 kJ/mol or more negative are associated with sharing or transfer of electrons from organic inhibitor molecules to the metal surface forming coordinate type bond (chemisorption) [32].

The absolute values of ΔG_{ads}^0 are both around 37 kJ/mol. This confirms that the adsorption of APTT and ANTT on copper surface may involve complex interactions: both physical adsorption and chemical adsorption [33]. The possible adsorption mechanism is [34, 35]: electrostatic interaction between the charged inhibitor molecules and charged copper surface. This process is called physical adsorption. Direct adsorption on the basis of donor-acceptor interactions between the lone pairs of electrons of heteroatoms, π -electrons of benzene and heterocyclic rings and the vacant orbitals of surface Cu atom is called chemical adsorption. Indirect adsorption of the charged inhibitor molecules on the copper surface through a synergistic effect with chloride ions from 3.5% NaCl solution, suggested that the adsorption of APTT and ANTT on copper surface involve physical as well as chemical adsorption.

3.4 SEM analyses

Fig. 8 presents a high-definition picture reflecting what happens on the interface (the SEM photographs of the copper specimens after immersed in 3.5% NaCl solution for 14 days at 303 K in the absence and presence of 100 mg/L inhibitors). The specimen surface in the absence of the inhibitors (Fig. 8 B) is strongly corroded, and the surface becomes porous and rough. In the presence of APTT and ANTT (Fig. 8 C and D), the surface of the specimens are well protected and the photographs are almost the same as that of the freshly polished surface (Fig. 8 A). These results indicate that a good protective adsorption film could be formed on the specimen surface, and the corrosion of copper in 3.5% NaCl solution is inhibited remarkably by the inhibitors. This is confirmed by EDX analysis. The EDX spectra in presence of APTT and ANTT show some peaks of nitrogen and sulfur. These peaks are due to nitrogen and sulfur of the adsorbed inhibitor species. This indicated that APTT and ANTT molecules were strongly adsorbed on the copper surface.

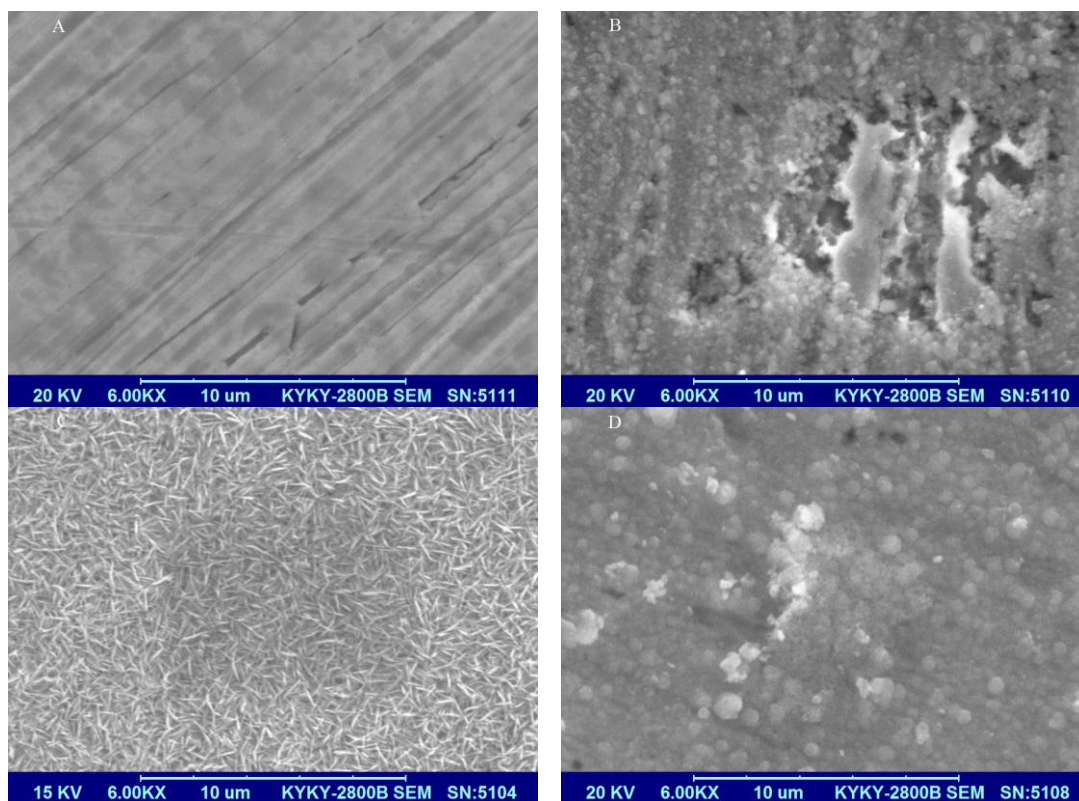


Figure 8. SEM image of (A) fresh polished copper and the copper surface obtained after 14 days immersion in 3.5% NaCl solution (B) without inhibitor, (C) with 100 mg/L APTT, (D) with 100 mg/L ANTT.

3.5 Quantum chemical calculation

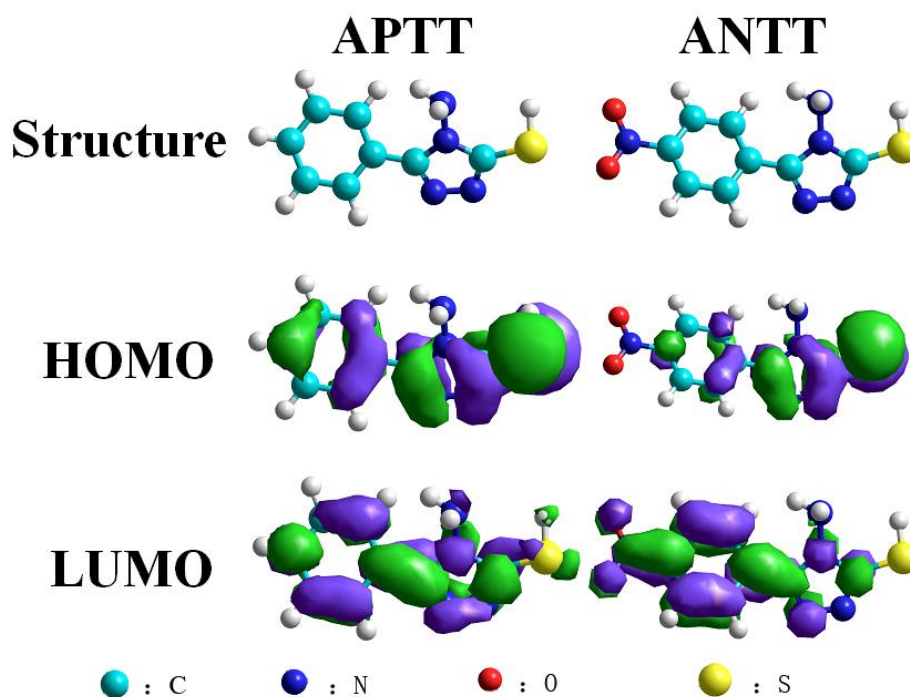


Figure 9. The full optimized minimum energy geometrical configurations and the frontier molecular orbital density distribution of APTT and ANTT

Table 6. Quantum chemical and dynamics parameters derived for APTT and ANTT.

	Total energy (kJ/mol)	E_{HOMO} (kJ/mol)	E_{LUMO} (kJ/mol)	ΔE (kJ/mol)	$I = -E_H$	$A = -E_L$	χ	η	ΔN
APTT	10486.8	-500.8	-119.6	381.2	500.8	119.6	310.2	190.6	0.401
ANTT	14516.1	-594.8	-109.9	484.9	594.8	109.9	352.4	242.5	0.228

The full optimized minimum energy geometrical configurations and the frontier molecular orbital density distribution of APTT and ANTT are shown in Fig.9. The computed quantum chemical properties such as E_{HOMO} , E_{LUMO} , ΔE_{H-L} , ionization potential (I), electron affinity (A) and fraction of transferred electrons (ΔN) are listed in the Table 6.

According to the frontier molecular orbital theory of chemical reactivity, transition of electron is due to an interaction between the frontier orbital, highest occupied molecular orbital (HOMO) and lowest unoccupied molecular orbital (LUMO) of reacting species. The energy of HOMO is directly related to the ionization potential and characterizes the susceptibility of the molecule toward attack by electrophiles [36,37]. The energy of LUMO is directly related to the electron affinity and characterizes the susceptibility of the molecule toward attack by nucleophiles. The lower the values of E_{LUMO} are, the stronger the electron accepting abilities of the molecules. The LUMO–HOMO gap is an important stability index. A large LUMO–HOMO gap implies high stability for the molecule in chemical reactions [22] a decrease of the energy gap usually leads to easier polarization of the molecule and adsorption on the surface. The results listed in Table 6 shows a smaller energy gap for APTT in comparison to ANTT.

The fraction of transferred electrons (ΔN) was calculated using the following equation [2,38]:

$$\Delta N = \frac{\chi_{Fe} - \chi_{inh}}{2(\eta_{Fe} + \eta_{inh})} \quad (15)$$

where χ_{Cu} and χ_{inh} denote the absolute electro negativity of copper and the inhibitor molecule, respectively; η_{Cu} and η_{inh} denote the absolute hardness of copper and the inhibitor molecule, respectively. These quantities are related to electron affinity (A) and ionization potential (I) as follows:

$$\chi = (I+A)/2 \quad (16)$$

$$\eta = (I-A)/2 \quad (17)$$

In order to calculate the fraction of electrons transferred, a theoretical value for the absolute electronegativity of copper according to Pearson was used $\chi_{Cu} = 463.1$ kJ/mol [39], and a global hardness of $\eta_{Cu} = 0$, by assuming that for a metallic bulk $I = A$ [40] because they are softer than the neutral metallic atoms.

In literature, it has been reported that the values of ΔN show inhibition effect resulted from electrons donation [38,39]. According to Lukovits's study [38], if the value of $\Delta N < 3.6$, the inhibition efficiency increased with increasing electron donating ability of inhibitor at the metal surface [41]. Also it was observed that inhibition efficiency increased with increase in the values of ΔN .

From Table 6, it is possible to observe that molecule APTT has a lower value of global hardness. The fraction of transferred electrons is also larger for molecule APTT and, in turn, is ANTT. The calculated results are in agreement with experimental results.

4. CONCLUSIONS

In the presence of APTT and ANTT, the corrosion of freshly polished copper in synthetic seawater (3.5% NaCl solution) is reduced effectively. The morphology of the specimen surface is provided by SEM. The inhibition efficiencies increase with the concentration enhancement of the inhibitors. The values of the inhibition efficiency obtained from the polarization curves are 95.1% and 91.2% respectively at 100 mg/L concentration, which are in good agreement with the data obtained from EIS (95.3% and 91.5 respectively). Polarization curves suggest that APTT and ANTT belong to mixed-type inhibitors, and the cathodic suppression plays a dominant role. EIS results indicate that the good inhibition performance attributes to the protective adsorption film of the compounds formed on copper surface. Thermodynamic calculation reveals that the adsorption follows well the Langmuir isotherm and the weak chemisorption is involved in the interaction between inhibitors and the copper surface. Thus, our research demonstrates that APTT and ANTT have great potentials as copper inhibitors.

ACKNOWLEDGEMENTS

The author gratefully acknowledges the support of National Nature Science Foundation of China (51179182), Provincial Science Foundation for Distinguished Young Scholars of Shandong (JQ201217), Shinan Scientific and Technological R&D Foundation of Qingdao City, China (2010-4-18-ZH) and K.C.Wong Education Foundation, Hong Kong.

References

1. L. Núñez, E. Reguera, F. Corvo, E. González, C. Vazquez, *Corros. Sci.* 47 (2005), pp. 461-484.
2. K.F. Khaled, *Mater. Chem. Phys.* 112 (2008) 104-111.
3. E.M. Sherif, *Appl. Surf. Sci.* 252 (2006) 8615-8623.
4. G. Trabanelli, *Corrosion* 47 (1991) 410-419.
5. H.O. Curkovic, E. Stupnisek-Lisac, H. Takenouti, *Corros. Sci.* 51 (2009) 2342-2348.
6. A. Dermaj, N. Hajjaji, S. Joiret, K. Rahmounia, A. Srhiri, H. Takenouti, V. Vivier, *Electrochim. Acta* 52 (2007) 4654-4662.
7. K. Rahmounia, N. Hajjaji, M. Keddama, A. Srhiri, H. Takenouti, *Electrochim. Acta* 52 (2007) 7519-7528.
8. M. Scendo, *Corros. Sci.* 50 (2008) 1584-1592.
9. S. Varvara, L.M. Muresan, K. Rahmouni, H. Takenouti, *Corros. Sci.* 50 (2008) 2596-2604.

10. E. Stupnišek-Lisac, A. Gazivoda, M. Madžarac, *Electrochim. Acta* 47 (2002) 4189-4194.
11. H. Ashassi-Sorkhabi, E. Asghari, *Electrochim. Acta* 54 (2008) 162-167.
12. K. Es-Salah, M. Keddou, K. Rahmouni, A. Srhiri, H. Takenouti, *Electrochim. Acta* 49 (2004) 2771-2778.
13. E.M. Sherif, R.M. Erasmus, J.D. Comins, *J. Colloid Interface Sci.* 309 (2007) 470-477.
14. E. Szöcs, G. Vastag, A. Shaban, E. Kálmán, *Corros. Sci.* 47 (2005) 893-908.
15. E.M. Sherif, S.M. Park, *Corros. Sci.* 48 (2006) 4065-4079.
16. K.M. Ismail, *Electrochim. Acta* 52 (2007) 7811-7819.
17. A. Dafali, B. Hammouti, R. Mokhlisse, S. Kertit, *Corros. Sci.* 45 (2003) 1619-1630.
18. H. Otmačić, E. Stupnišek-Lisac, *Electrochim. Acta* 48 (2003) 985-991.
19. S.S.A. El-Rehim, M.A.M. Ibrahim, K.F. Khaled, *J. Appl. Electrochem.* 29 (1999) 593-599.
20. W.H. Li, L.C. Hu, S.T. Zhang, B.R. Hou, *Corros. Sci.* 53 (2011) 735-745.
21. Y. Yan, W. Li, L. Cai, B. Hou, *Electrochim. Acta* 53 (2008) 5953-5960.
22. S. Zhang, Z. Tao, W. Li, B. Hou, *Appl. Surf. Sci.* 255 (2009) 6757-6763.
23. T. Szauer, A. Brandt, *Electrochim. Acta* 26 (1981) 1209-1217.
24. N.M. Guan, L. Xueming, L. Fei, *Mater. Chem. Phys.* 86 (2004) 59-68.
25. X.H. Li, S.D. Deng, H. Fu, *Corros. Sci.* 53 (2011) 664-670.
26. M. Sahin, S. Bilgic, H. Yilmaz, *Appl. Surf. Sci.* 195 (2002) 1-7.
27. A.K. Singh, M.A. Quraishi, *Corros. Sci.* 51 (2009) 2752-2760.
28. B. Ateya, B. El-Anadawi, F. El-Nizamy, *Corros. Sci.* 24 (1984) 509-515.
29. J.M. Cases, F. Villieras, *Langmuir* 8 (1992) 1251-1264.
30. J. Flis, T. Zakroczyński, *J. Electrochem. Soc.* 143 (1996) 2458-2464.
31. F. Bentiss, M. Lebrini, M. Lagrenée, *Corros. Sci.* 47 (2005) 2915-2931.
32. F.M. Donahue, K. Nobe, *J. Electrochem. Soc.* 112 (1965) 886-891.
33. W. Li, Q. He, S. Zhang, C. Pei, B. Hou, *J. Appl. Electrochem.* 38 (2008) 289.
34. I. Ahmad, R. Prasad, M.A. Quraishi, *Corros. Sci.* 52 (2010) 933-942.
35. D.P. Yadav, B. Maiti, M.A. Quraishi, *Corros. Sci.* 52 (2010) 3586-3598.
36. M.A. Amin, M.A. Ahmed, H.A. Arida, F. Kandemirli, M. Saracoglu, T. Arslan, M.A. Basaran, *Corros. Sci.* 53 (2011) 1895-1909.
37. N.O. Obi-Egbedi, I.B. Obot, *Corros. Sci.* 53 (2011) 263-275.
38. I. Lukovits, E. Kalman, F. Zucchi, *Corrosion* 57 (2001) 3.
39. V.S. Sastri, J.R. Perumareddi, *Corros. Sci.* 53 (1997) 617-622.
40. R. Valdez, L.M. Martinez-Villafane, D. Glossman-Mitnik, *J. Mol. Struct.: Theochem* 716 (2005) 61-65.
41. G. Gece, S. Bilgic, *Corros. Sci.* 52 (2010) 3304-3308.